XA0202020

Test of RIPL-2 cross section calculations

M. Herman
International Atomic Energy Agency, Vienna, Austria

29th November 2001

The new levels and optical segments and microscopic HF-BCS level densities (part of the density segment) were tested in practical calculations of cross sections for neutron induced reactions on 22 targets (40-Ca, 47 -Ti, 52-Cr, 55-Mn, 58-Ni, 63-Cu, 71-Ga, 80-Se, 92-Mo, 93-Nb, 100-Mo, 109-Ag, 114-Cd, 124-Sn, 127-I, 133-Cs, 140-Ce, 153-Eu, 169-Tm, 186-W, 197-Au, 208-Pb). For each target all reactions involving up to 3 neutron, 1 proton and 1 α-particle emissions (subject to actual reaction thresholds) were considered in the incident energy range from 1 keV up to 20 MeV (in some cases up to 27 MeV). In addition, total, elastic, and neutron capture cross sections were calculated.

The 2-17beta version of the statistical model code EMPIRE-II has been used with all default parameters except of those differentiating the 3 series of runs. In all cases TUL MSD and Heidelberg MSC models were used for preequilibrium emission of neutrons, and exciton model (DEGAS) for preequilibrium emission of protons and γ's. These were complemented with Hauser-Feshbach calculations including widths fluctuations (HRTW model) at incident energies below 5 MeV. The results were converted into the ENDF-6 format and compared with experimental data available from the EXFOR library.

The aim of this exercise was to test formal correctness and performance of the new file with discrete levels provided by Belgya, Koning's global optical model potentials and microscopic level densities provided by Goriely. Accordingly, the following three series of calculations were performed:

standard default parameters in EMPIRE-2-17beta (i.e., Wilmore-Hodgson omp for neutrons and Becchetti-Greenlees for protons, EMPIRE-specific level densities with internal systematics, and internal library of discrete levels with N_{max} set arbitrarily to 10)

Ko-Be Koning's optical model potential for neutrons and protons, Belgya's file of discrete levels with recommended N_{max} (limited to 40 by the ENDF-6 format), and EMPIRE specific level densities

Ko-Be-Go as above but using HF-BCS microscopic level densities provided by Goriely instead of EMPIRE-specific ones

Typical plots comparing results obtained in the three runs are shown in Figs.1-22. General conclusions resulting form this exercise are following:

- No problems were encountered while processing the new RIPL-2 files. This indicates that there are no fatal formatting errors that would prevent files from being used in cross section calculations.
- Comparison with the experimental data shows reasonable overall agreement for all three series of calculations. No clear 'winner' could be declared since for each data set there are reactions for which this set is the best. However, general preference goes to the Ko-Be set, which demonstrates improvement brought about by RIPL-2.

- HF-BCS microscopic level densities were found to perform comparable to the phenomenological level densities and in some cases appear to be clearly the best (e.g., ^{58}Ni(n,p) reaction cross sections and double-differential cross sections for neutron production on ^{93}Nb at 14 MeV). On the other hand, microscopic level densities tend to overestimate capture cross sections in certain number of cases.
- Significant discrepancies among the results of the three sets of calculations were observed in several cases. Taking into account that none of the sets can be considered as absolutely superior we have to accept that a set of parameters which would be 'universally the best' can not be recommended.

The results of the present comparison, although short of completeness, stress importance of the model parameters and prove practical usefulness of the RIPL-2 library for applications and basic research.

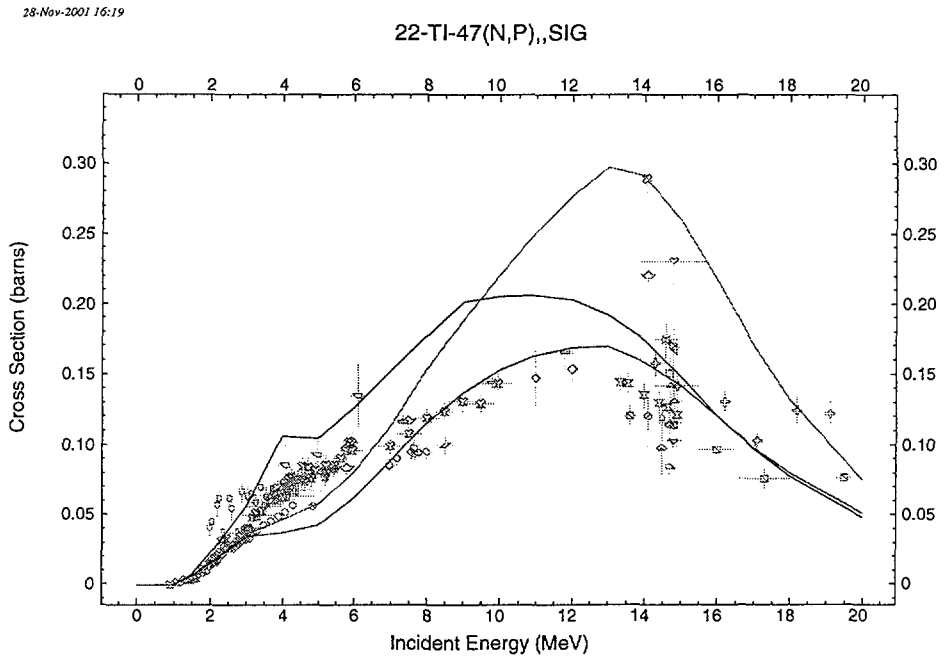

Figure 1: Comprison of experimental data with results calculated using three sets of parameters (see text) for the ^{47}Ti(n,p) reaction.

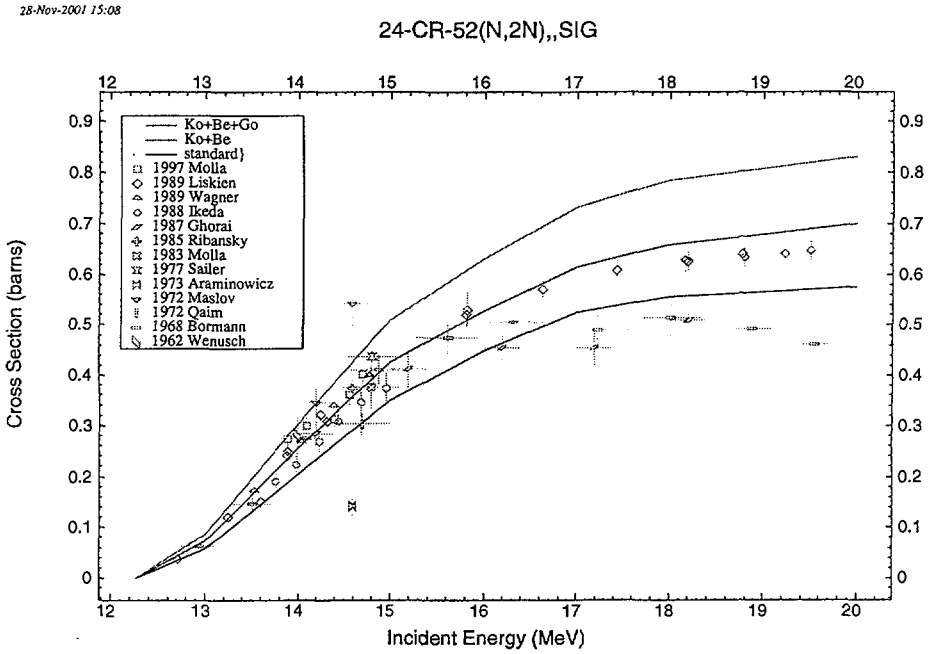

Figure 2: Comprison of experimental data with results calculated using three sets of parameters (see text) for the ^{52}Cr(n,2n) reaction.

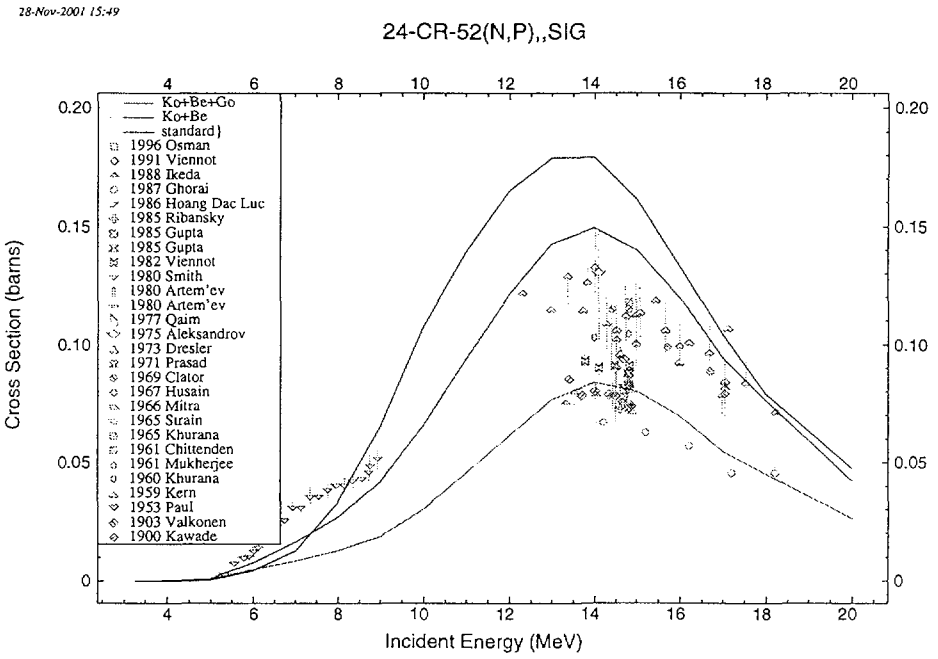

Figure 3: Comprison of experimental data with results calculated using three sets of parameters (see text) for the ^{52}Cr(n,p) reaction.

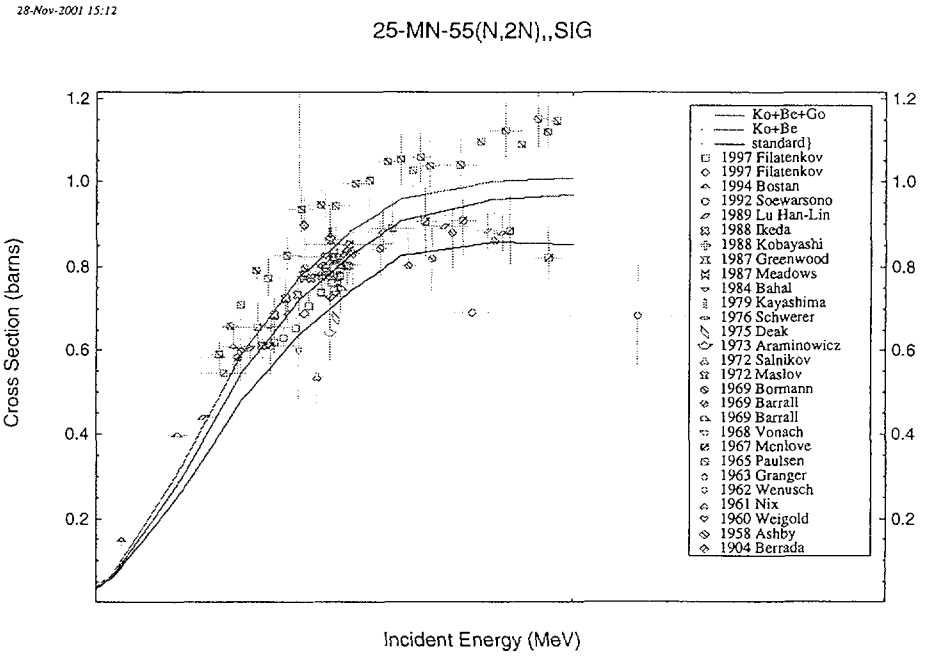

Figure 4: Comprison of experimental data with results calculated using three sets of parameters (see text) for the ^{55}Mn(n,2n) reaction.

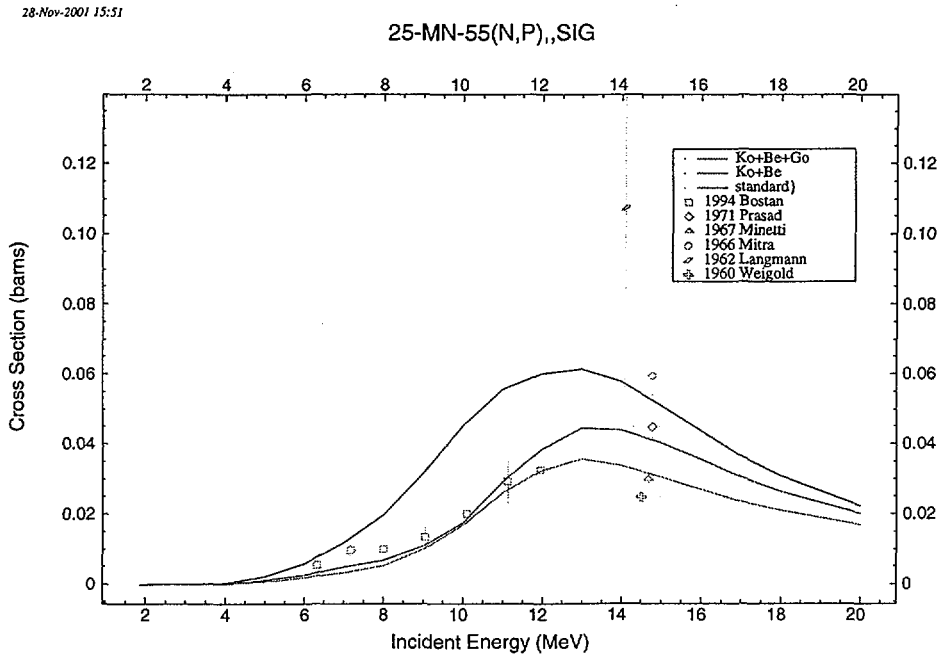

Figure 5: Comprison of experimental data with results calculated using three sets of parameters (see text) for the ^{55}Mn(n,p) reaction.

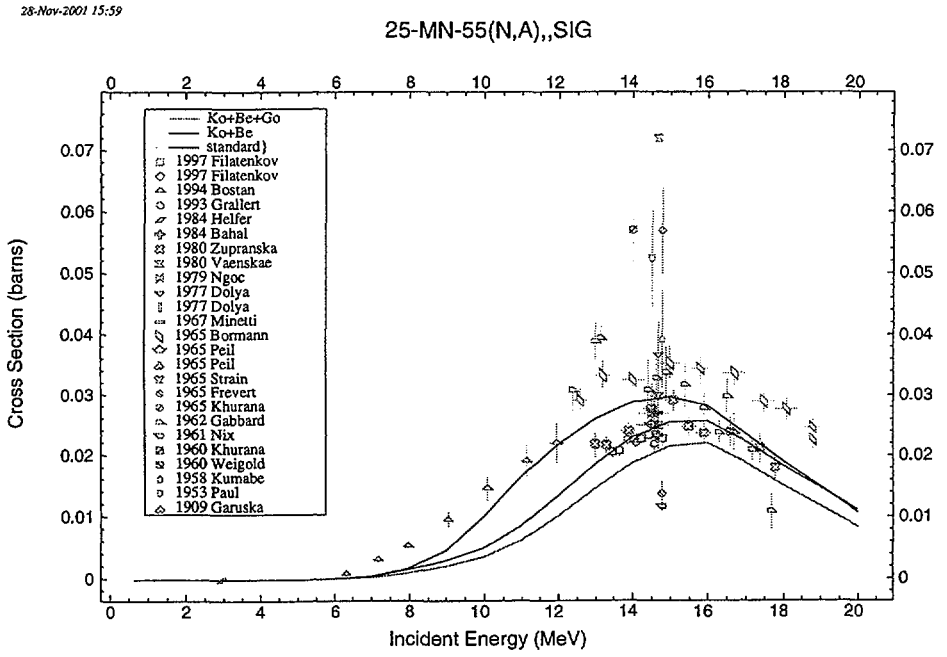

Figure 6: Comprison of experimental data with results calculated using three sets of parameters (see text) for the ^{55}Mn(n,α) reaction.

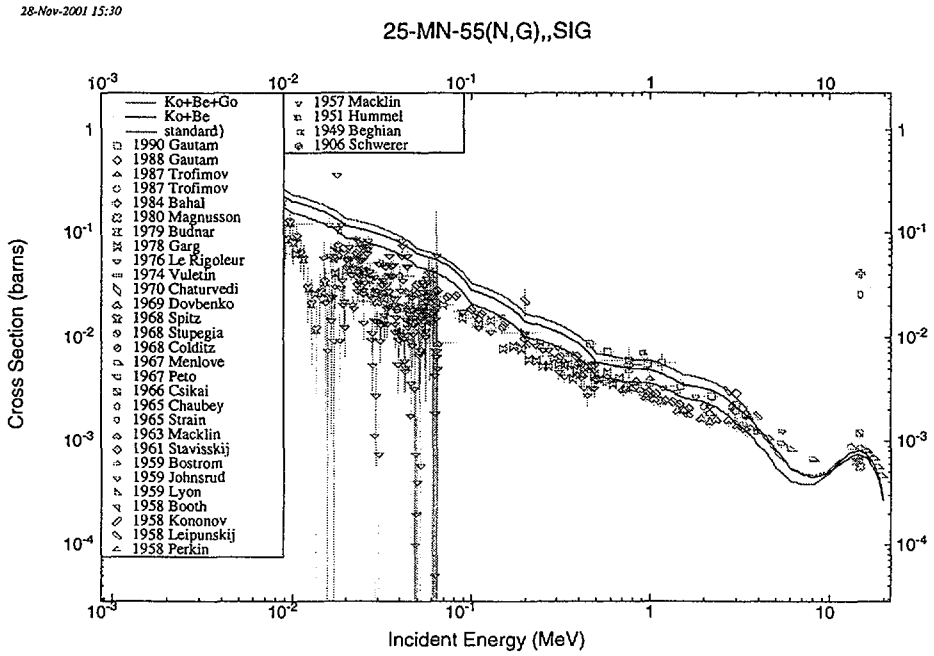

Figure 7: Comprison of experimental data with results calculated using three sets of parameters (see text) for the ^{55}Mn(n,γ) reaction.

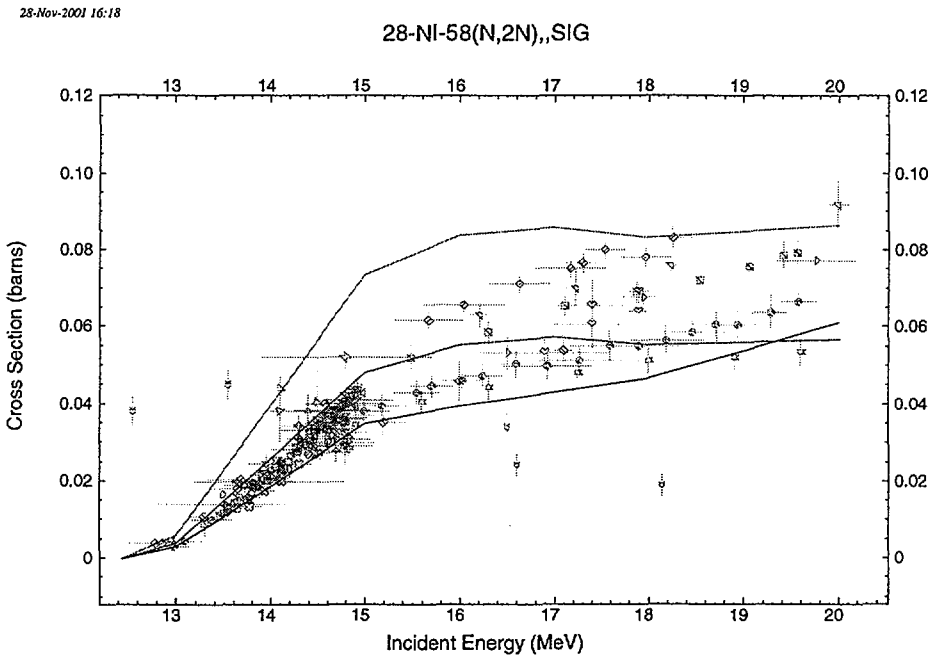

Figure 8: Comprison of experimental data with results calculated using three sets of parameters (see text) for the ^{58}Ni(n,2n) reaction.

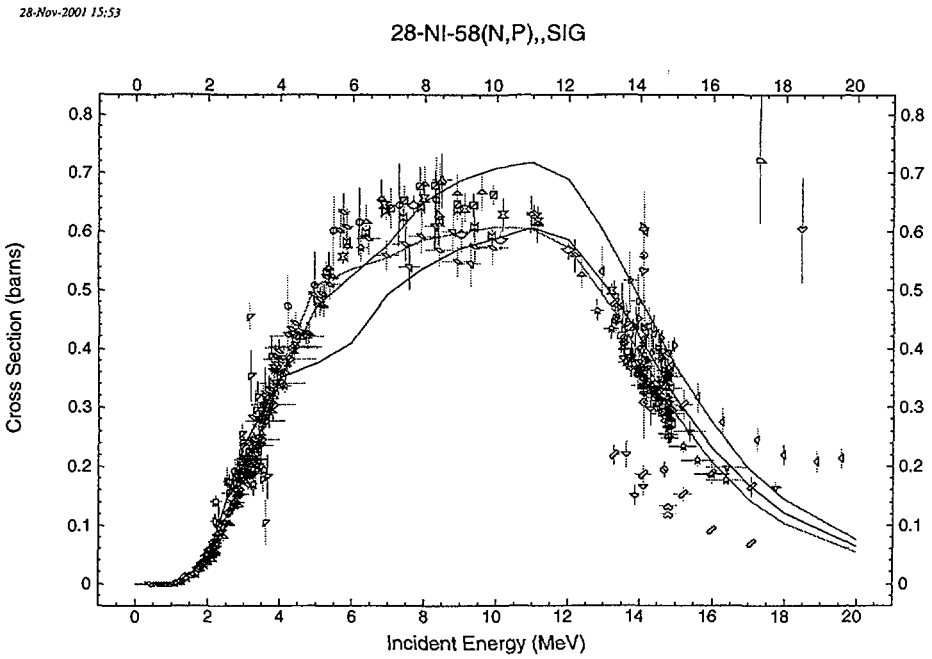

Figure 9: Comprison of experimental data with results calculated using three sets of parameters (see text) for the ^{58}Ni(n,p) reaction.

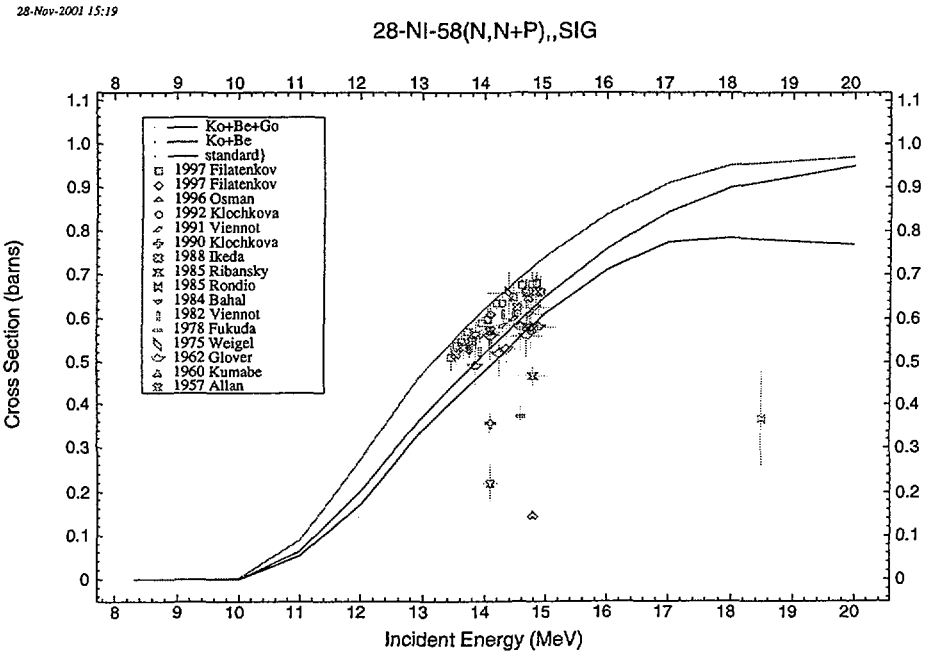

Figure 10: Comprison of experimental data with results calculated using three sets of parameters (see text) for the ^{58}Ni(n,np) reaction.

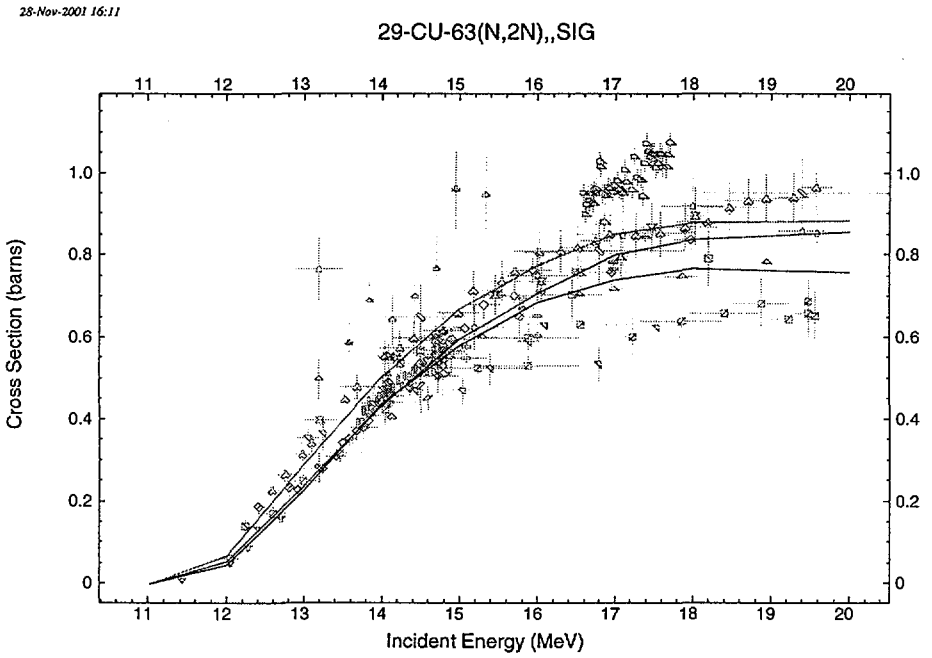

Figure 11: Comprison of experimental data with results calculated using three sets of parameters (see text) for the ^{63}Cu(n,2n) reaction.

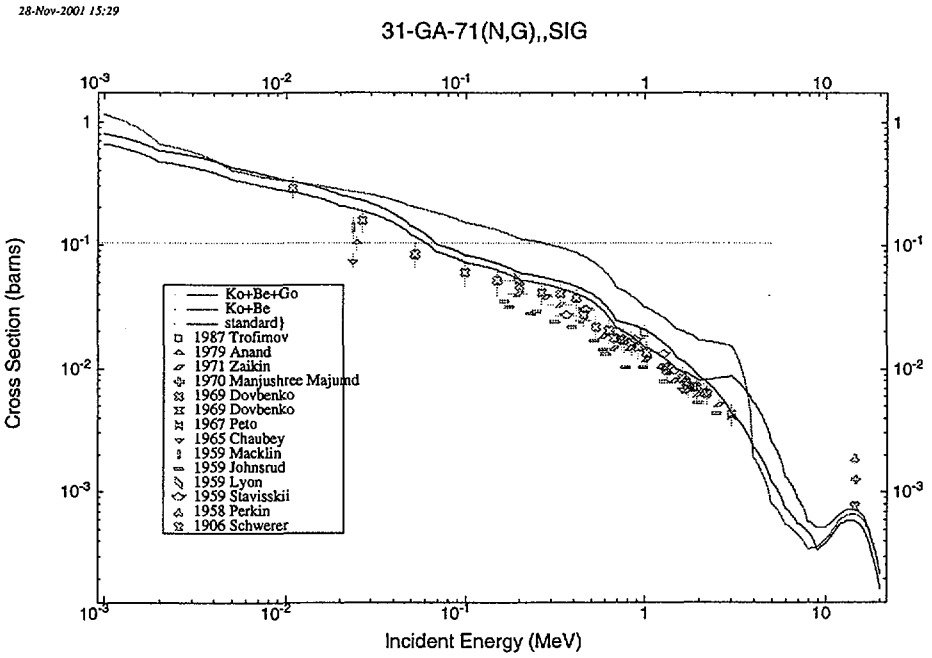

Figure 12: Comprison of experimental data with results calculated using three sets of parameters (see text) for the ^{71}Ga(n,γ) reaction.

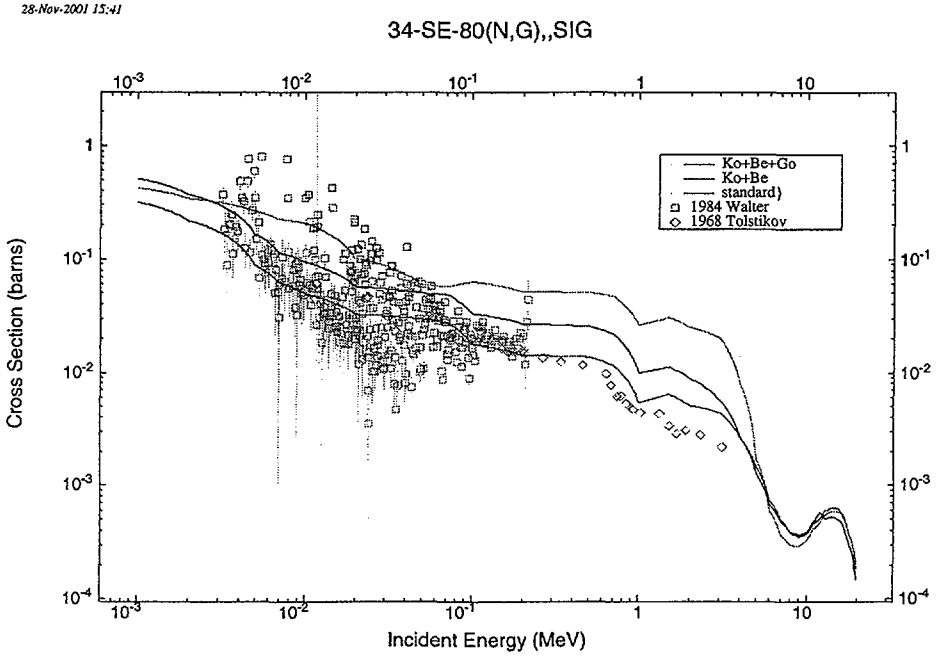

Figure 13: Comprison of experimental data with results calculated using three sets of parameters (see text) for the ^{80}Se(n,γ) reaction.

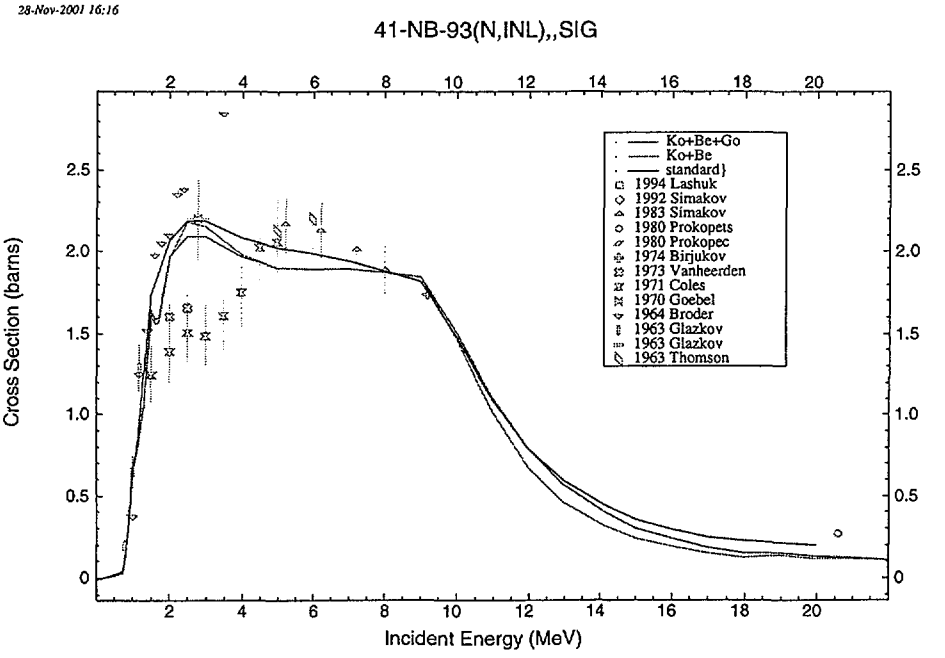

Figure 14: Comprison of experimental data with results calculated using three sets of parameters (see text) for the ^{93}Nb(n,inl) reaction.

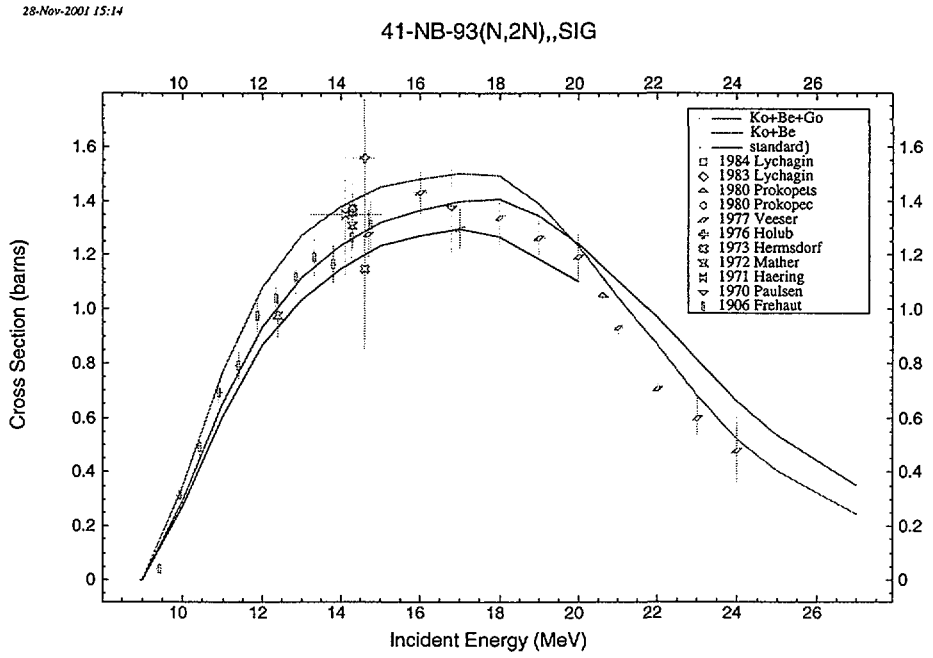

Figure 15: Comprison of experimental data with results calculated using three sets of parameters (see text) for the ^{93}Nb(n,2n) reaction.

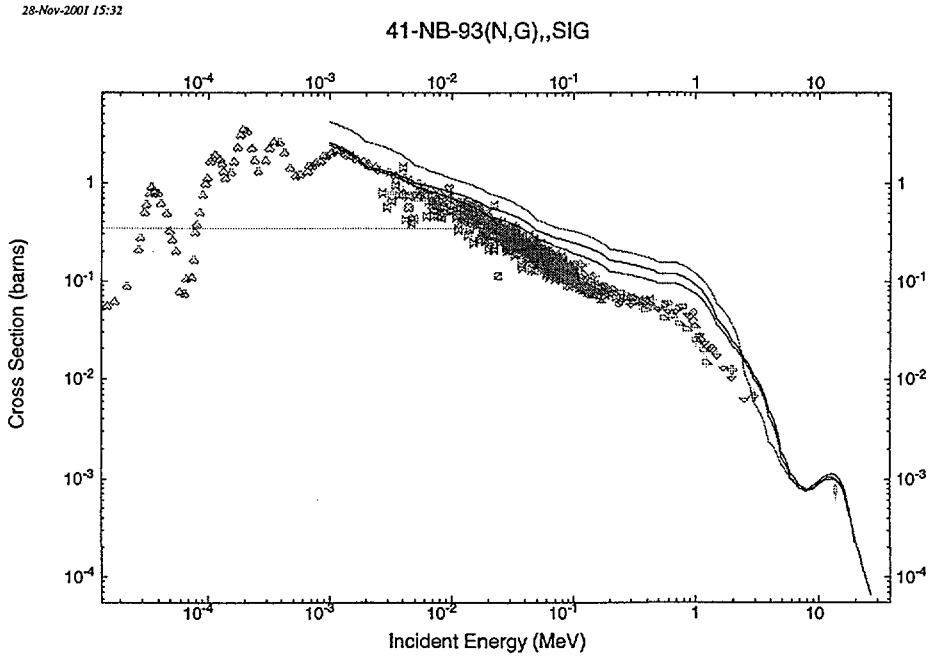

Figure 16: Comprison of experimental data with results calculated using three sets of parameters (see text) for the ^{93}Nb(n,γ) reaction.

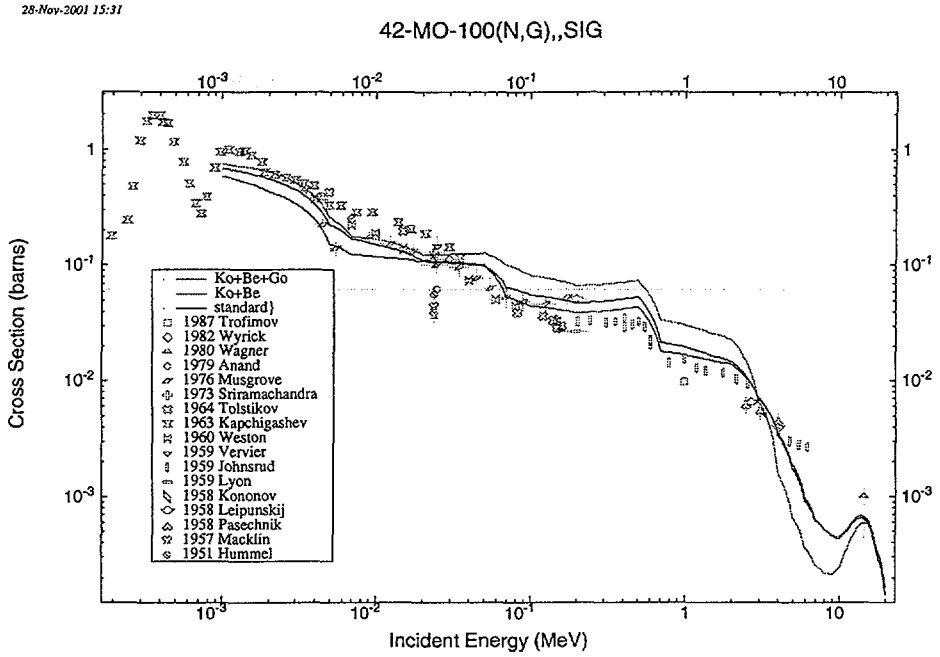

Figure 17: Comprison of experimental data with results calculated using three sets of parameters (see text) for the ^{100}Mo(n,γ) reaction.

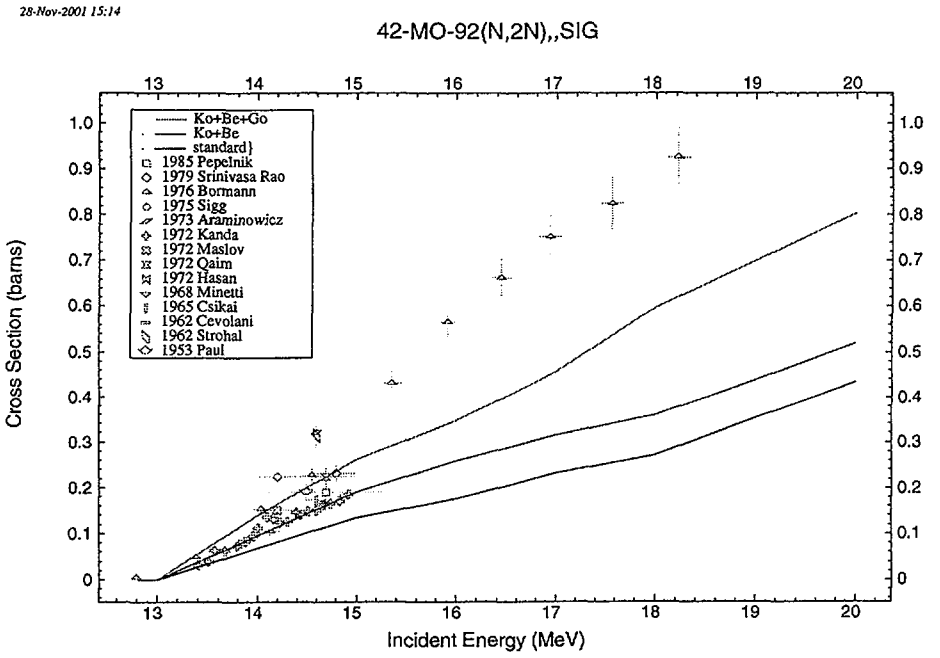

Figure 18: Comprison of experimental data with results calculated using three sets of parameters (see text) for the ^{92}Mo(n,2n) reaction.

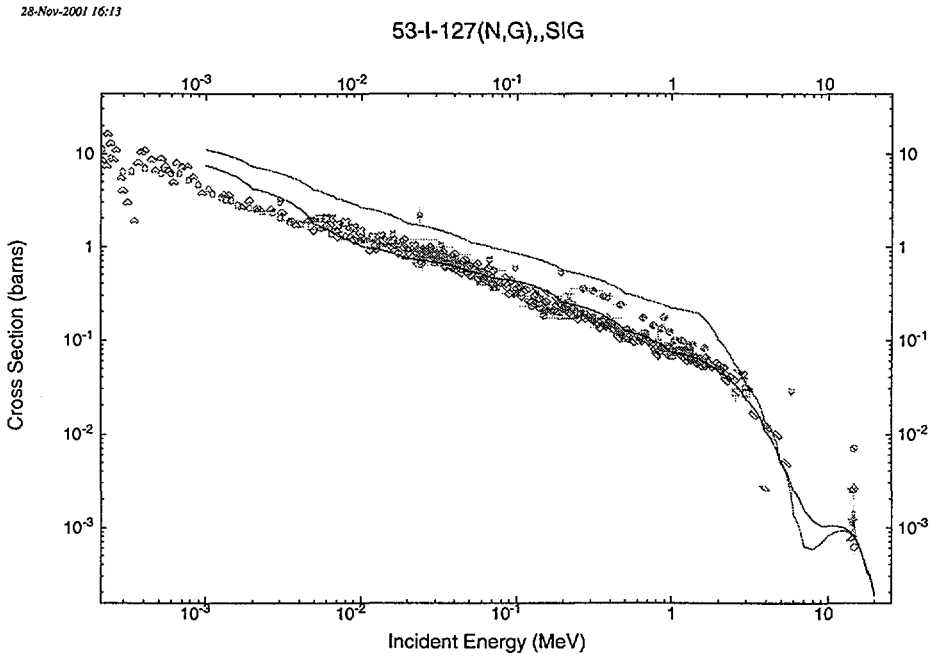

Figure 19: Comprison of experimental data with results calculated using three sets of parameters (see text) for the ^{127}I(n,γ) reaction.

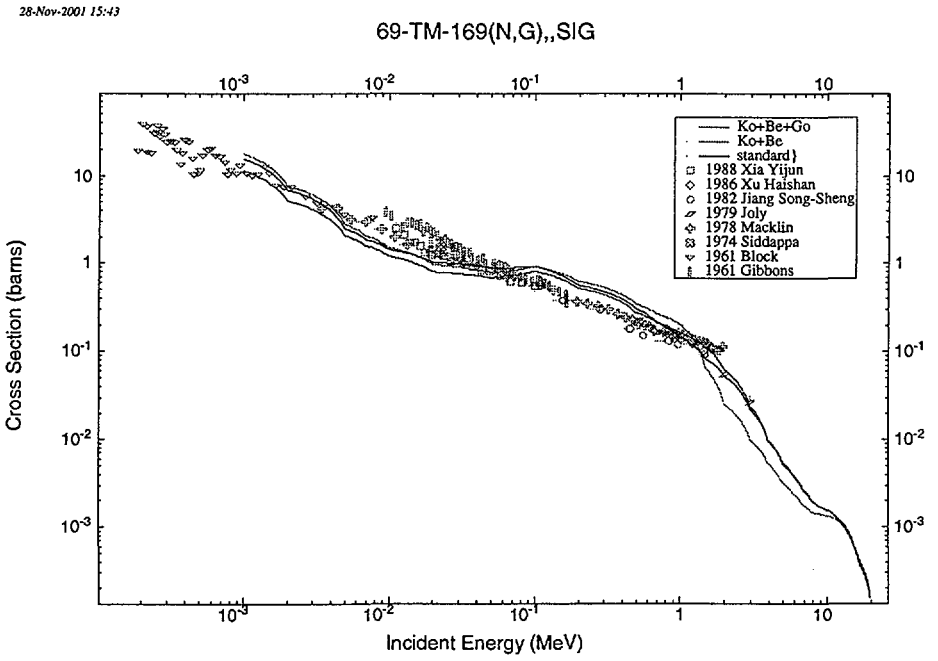

Figure 20: Comprison of experimental data with results calculated using three sets of parameters (see text) for the ^{169}Tm(n,γ) reaction.

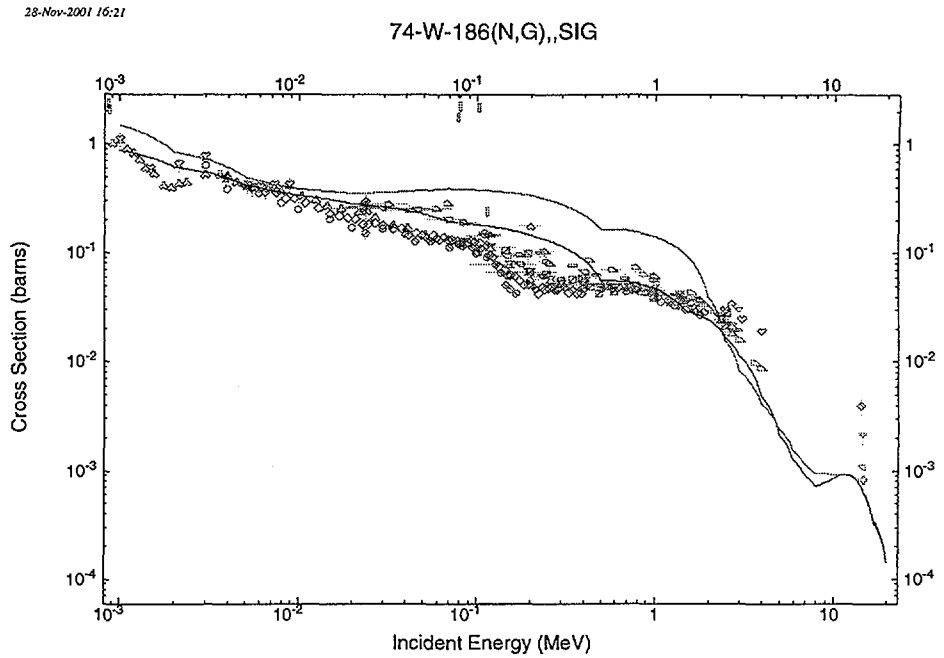

Figure 21: Comprison of experimental data with results calculated using three sets of parameters (see text) for the ^{186}W(n,γ) reaction.

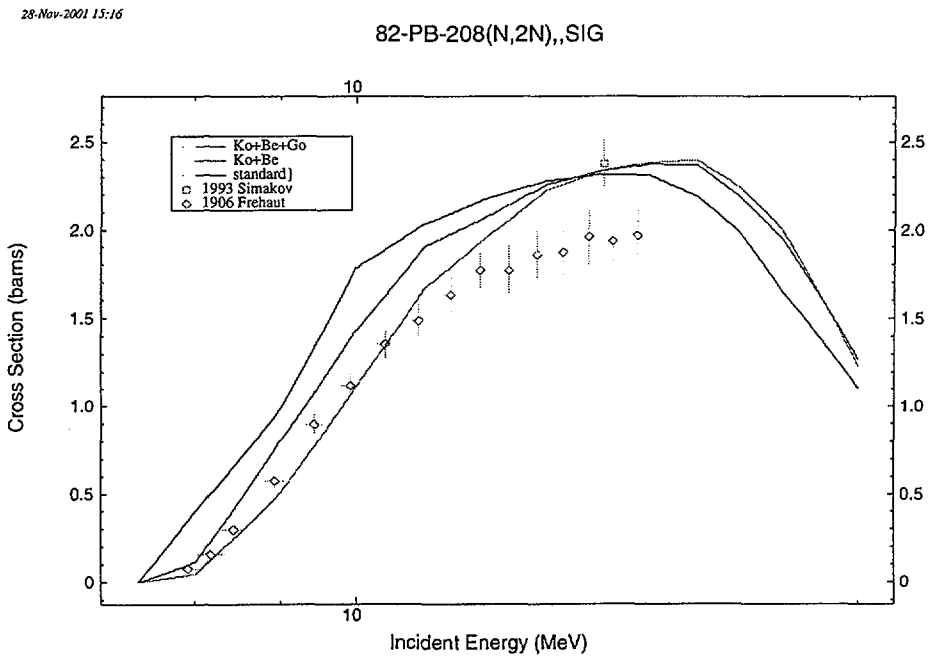

Figure 22: Comprison of experimental data with results calculated using three sets of parameters (see text) for the ^{208}Pb(n,2n) reaction.

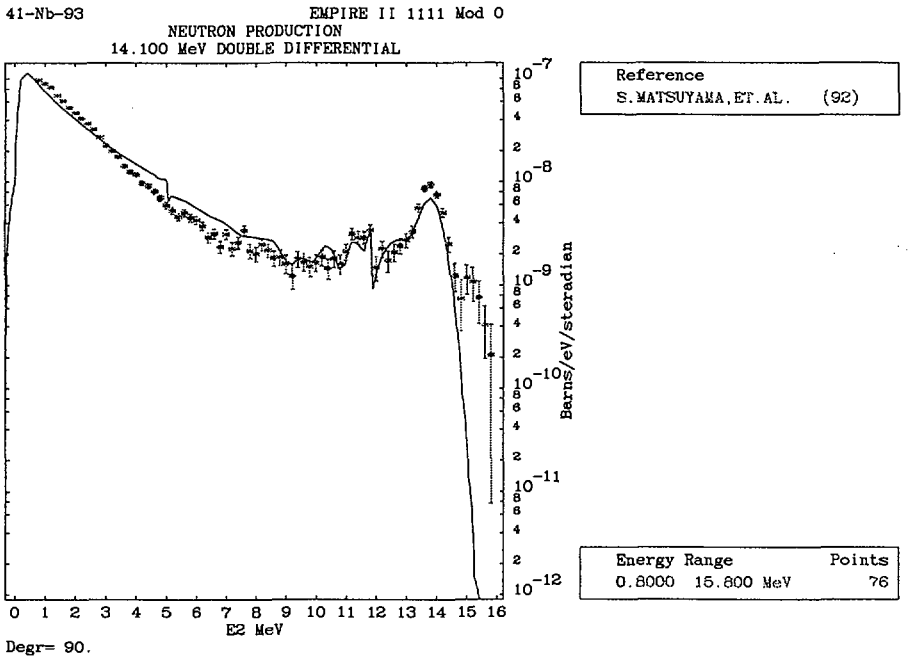

Figure 23: Experimental double-differential cross sections for neutron production on ^{93}Nb compared with theoretical results calculated with the Ko-Be set of parameters.

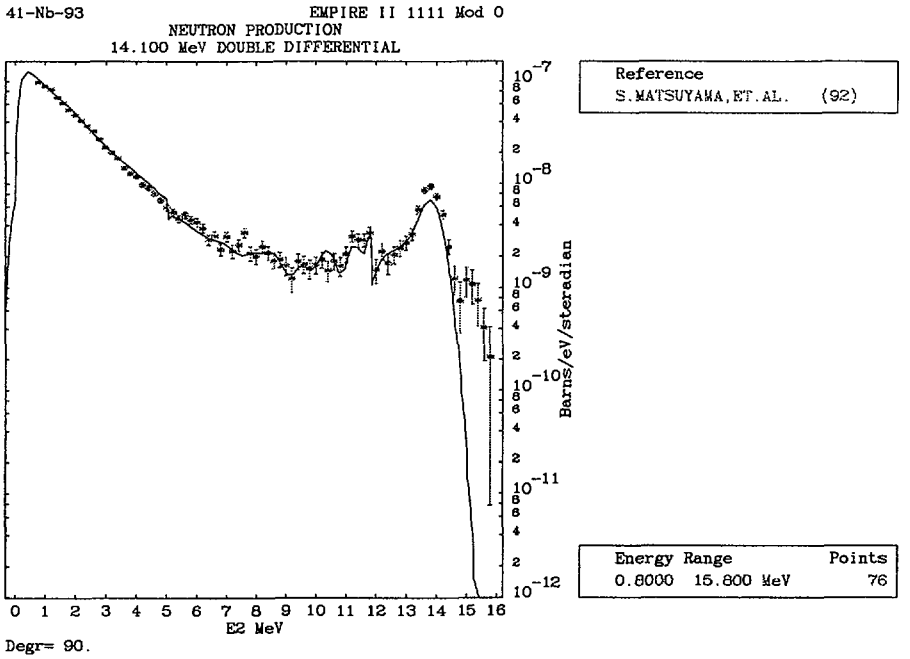

Figure 24: Experimental double-differential cross sections for neutron production on ^{93}Nb compared with theoretical results calculated with the Ko-Be-Go set of parameters. Compare to the plot above.